

# LUMINOSITY EFFECTS DUE TO DEPENDENT HEAVY-TAILED BEAMS

E. Lamb<sup>\*1</sup>, H. Bartosik, G. Sterbini, CERN, Meyrin, Switzerland  
<sup>1</sup>also at EPFL, Lausanne, Switzerland

## Abstract

The luminosity of particle colliders depends, among other parameters, on the transverse profiles of the colliding beams. At the LHC at CERN, heavy-tailed transverse beam distributions are typically observed in routine operation. The luminosity is usually modelled with the assumption that the  $x$ - $y$  planes are independent (i.e. statistically uncorrelated particle distributions between the planes) in each beam. Analytical calculations show that the solution of inverting 1D heavy-tailed beam profiles to transverse 4D phase-space distributions is not unique. For a given transverse beam profile, the distributions can be dependent (i.e. statistically correlated) or independent in the transverse planes, even in the absence of machine coupling. In this work, the effect of transverse  $x$ - $y$  dependence of the 4D phase space distribution on the luminosity of a particle collider is evaluated for heavy-tailed beams.

## INTRODUCTION

During the operation of accelerators, it is important to control the beam profile, e.g. to minimize beam losses or optimise the luminosity of colliders. The beam profile is a projection of the total distribution onto one plane. For example, a wire scanner can measure the transverse distribution in the horizontal or in the vertical plane. Mathematically, this is equivalent to performing the integral of the beam distribution over the other planes of the phase space. For example, assuming a 4D phase space distribution  $f_{4D}(x, p_x, y, p_y)$  the profile in the horizontal plane is obtained as:

$$f_{1D}(x) = \int_{-\infty}^{\infty} \int_{-\infty}^{\infty} \int_{-\infty}^{\infty} f_{4D}(x, p_x, y, p_y) dp_x dy dp_y,$$

where we consider a distribution with the normalisation condition:

$$\int_{-\infty}^{\infty} \int_{-\infty}^{\infty} \int_{-\infty}^{\infty} \int_{-\infty}^{\infty} f_{4D}(x, p_x, y, p_y) dx dp_x dy dp_y = 1. \quad (1)$$

If only the profile  $f_{1D}(x)$  is known, and we want to invert it to find the 4D phase space distribution, the solution is not unique. The only constraints are that the projection of  $f_{4D}(x, p_x, y, p_y)$  must match the observed  $f_{1D}(x)$ . In addition, the distribution  $f_{2D}(x, p_x)$  and  $f_{2D}(y, p_y)$  need to be circularly symmetric in the action-angle space, (normalised phase space), in order for the distribution to be matched to the Hamiltonian of the system. In recent work it was shown experimentally how correlations in the 6D phase space can be introduced via space charge induced periodic crossing of coupled resonances [1].

\* eleanor.rose.lamb@cern.ch

## INVERSION OF BEAM PROFILES

From an observed beam profile, we can get the radial distribution of the canonical phase space variables using the Abel transform [2, 3]. To find the beam distribution in a higher dimension we could impose one of the following additional constraints,

1. circular symmetry (i.e. round distributions in  $x$ - $y$ ),
2. forcing the transverse planes to be factorizable.

For case 1, imposing circular symmetry in all planes, we define the following variables, or radii, from the canonical variables:

$$r_x = \sqrt{x^2 + p_x^2}, \quad (2)$$

$$r_y = \sqrt{y^2 + p_y^2}, \quad (3)$$

$$s = \sqrt{x^2 + p_x^2 + y^2}, \quad (4)$$

and a 4D ‘super-radius’:

$$m = \sqrt{r_x^2 + r_y^2} = \sqrt{x^2 + p_x^2 + y^2 + p_y^2}. \quad (5)$$

To find  $f_{2D}(r_x)$ , the Abel transform is applied once on  $f_{1D}(x)$ . To find  $f_{4D}(m)$ , and the inverse Abel transform is applied three times to  $f_{1D}(x)$  in accordance with the property of extension to higher dimensions. Thus, any 4D distribution can be found given that the inverse Abel transform is real for an  $f_{1D}(x)$ . The constraint is however that the normalised (with respect to emittance) distributions are the same in  $x$  and  $y$ .

Starting from a projection in 1D, e.g. in  $x$ ,  $f_{1D}(x)$ , we obtain

$$f_{2D}(r_x) = -\frac{1}{\pi} \int_r^{\infty} \frac{df_{1D}(x)}{dx} \frac{dx}{\sqrt{x^2 - r_x^2}}, \quad (6)$$

$$f_{3D}(s) = -\frac{1}{\pi} \int_s^{\infty} \frac{df_{2D}(r_x)}{dr_x} \frac{dr_x}{\sqrt{r_x^2 - s^2}}, \quad (7)$$

$$f_{4D}(m) = -\frac{1}{\pi} \int_m^{\infty} \frac{df_{3D}(s)}{ds} \frac{ds}{\sqrt{s^2 - m^2}}, \quad (8)$$

This is equivalent to

$$f_{4D}(m) = \mathcal{A}^{-1}[\mathcal{A}^{-1}[\mathcal{A}^{-1}[f_{1D}(x)]]], \quad (9)$$

where  $\mathcal{A}$  is the Abel transform. Conversely, we can compute the 1D distribution from a given 4D with forward Abel transforms, equivalent to a Cartesian integration in  $dp_x dp_y dy$ ,

$$\begin{aligned} f_{1D}(x) &= \mathcal{A}[\mathcal{A}[\mathcal{A}[f_{4D}(m)]]] \\ &= \int_{-\infty}^{\infty} \int_{-\infty}^{\infty} \int_{-\infty}^{\infty} f_{4D}(m) dy dp_y dp_x. \end{aligned} \quad (10)$$

If we have a distribution function in 4D which is a function of  $m$ , the beam is matched and stationary, as  $m$  depends on the canonical variables.

### Gaussian Distribution

For Gaussian  $f_{1D}(x)$  profiles, the  $f_{4D}(m)$  for a round distribution in  $x - y$  is trivially found, and is identical to the case of a “factorizable” constraint, as the distribution can be split into parts corresponding to  $x$  and  $y$ , with  $m_0$  a constant which can be changed depending on the specific distribution:

$$\begin{aligned} f_{4D}(m) &= \frac{1}{\pi^2 m_0^4} \exp\left(-\frac{m^2}{m_0^2}\right) \\ &= \frac{1}{\pi^2 m_0^4} \exp\left(-\frac{x^2 + p_x^2 + y^2 + p_y^2}{m_0^2}\right). \end{aligned} \quad (11)$$

### Waterbag and Parabolic Distributions

The use of the Abel transform to find axis-symmetric distributions can be validated on the waterbag and parabolic distributions, matching the 4D density functions given in [4].

Defining the 2D distribution  $f_{2D}(r_x)$  as waterbag yields:

$$f_{2D}(r_x) = \frac{2(1 - \frac{r_x^2}{m_0^2})}{\pi m_0^2}, \quad (12)$$

$$f_{3D}(s) = \mathcal{A}^{-1}[f_{2D}(r_x)] = \frac{4\sqrt{m_0^2 - s^2}}{\pi^2 m_0^4}, \quad (13)$$

$$f_{4D}(m) = \mathcal{A}^{-1}[f_{3D}(s)] = \frac{2}{\pi^2 m_0^4}. \quad (14)$$

where  $m < m_0$  defines the region where the distribution is non-zero.

The case of a parabolic 2D  $f_{2D}(r_x)$  distribution yields:

$$f_{2D}(r_x) = \frac{1}{\pi m_0^2} 3\left(1 - \frac{r_x^2}{m_0^2}\right)^2, \quad (15)$$

$$f_{3D}(s) = \mathcal{A}^{-1}[f_{2D}(r_x)] = \frac{8(m_0^2 - s^2)^{3/2}}{\pi^2 m_0^6}, \quad (16)$$

$$f_{4D}(m) = \mathcal{A}^{-1}[f_{3D}(s)] = \frac{6(m_0^2 - m^2)}{\pi^2 m_0^6}. \quad (17)$$

It can be shown that these results are in agreement with [4].

### q-Gaussian

Beam profiles in the CERN accelerator complex have been observed to follow q-Gaussian distributions [5, 6]. We can find the q-Gaussian distribution function for the round symmetric case, starting from the 1D q-Gaussian [7]:

$$f_{1D}(x) = \frac{\sqrt{\beta_q}}{C_q} e_q(-\beta_q x^2), \quad (18)$$

where  $e_q(x) = [1 + (1 - q)x]_+^{\frac{1}{1-q}}$ ,  $q$  and  $\beta_q$  are the parameters of the q-Gaussian function, and  $C_q$  is a normalization constant. The variance of the distribution is given by:

$$\begin{aligned} &\frac{1}{\beta_q(5 - 3q)}, \text{ for } q < \frac{5}{3} \\ &\infty, \text{ for } \frac{5}{3} \leq q < 2 \end{aligned} \quad (19)$$

The 1D profile is transformed to a 2D density via the inverse Abel transform:

$$\begin{aligned} f_{2D}(r_x) &= -\frac{\beta_q^{3/2}(q-3)\sqrt{q-1}r_x}{2\pi} \\ &\times \left(\frac{1}{\beta_q(q-1)r_x^2} + 1\right)^{\frac{q+1}{2-2q}} \left(\beta_q(q-1)r_x^2\right)^{\frac{q}{1-q}}, \end{aligned} \quad (20)$$

Assuming a density in the form  $f_{4D}(m)$ , the equation for the 4D density function is obtained via two further inverse Abel transforms:

$$\begin{aligned} f_{4D}(m) &= -\frac{\beta_q(q-3)(q+1)\left(\frac{1}{\beta_q(q-1)}\right)^{\frac{1}{1-q}}}{4\pi^2 m^3 \Gamma\left(\frac{1}{q-1}\right)} \\ &\times (\beta_q(q-1))^{\frac{q+1}{2-2q}} \Gamma\left(\frac{q}{q-1}\right) \\ &\times \left(\frac{1}{\beta_q m^2(q-1)} + 1\right)^{\frac{1}{1-q} - \frac{3}{2}} (\beta_q m^2(q-1))^{\frac{1}{1-q}}, \end{aligned} \quad (21)$$

which is valid for the specific case of  $q$ -values of  $1 < q < 3$ . The function can be used to populate the phase space via a 4D Box-Müller [8] type inverse sampling method from [4]. The population of the phase space with a q-Gaussian of  $q = 1.4$  yields the  $x$ - $y$  projection shown in Fig. 1, which is elliptically symmetric. The projection on the  $x$  or  $y$  planes shows the histogram of the distribution and the fit of a q-Gaussian with  $q = 1.4$ . The densities for non-Gaussian beams with hyper-elliptic symmetry are non-factorizable. The solutions are however matched, as they are a function of  $m$  only.

In order to generate a particle distribution for factorizable distributions in  $x - y$  (case 2), the 4D density function is a product of two 2D density functions, one in  $x - p_x$  and one  $y - p_y$ , which are in themselves functions of only  $r_x$  and  $r_y$ . They can be found via one inverse Abel transform for each plane:

$$f_{4D}(r_x, r_y) = f_{2D}(r_x) \times f_{2D}(r_y). \quad (22)$$

The  $x - p_x$  and  $y - p_y$  distributions are then found via two separate Box-Müller type random sampling methods [8]. Figure 2 shows the projection of the density function made from the multiplication of two 2D distributions (case 2). The projection in  $x$ - $y$  has a characteristic cross shape, a consequence of the heavy tails and an independent distribution. As before, the projection in  $x$  and  $y$  fits the q-Gaussian distribution.

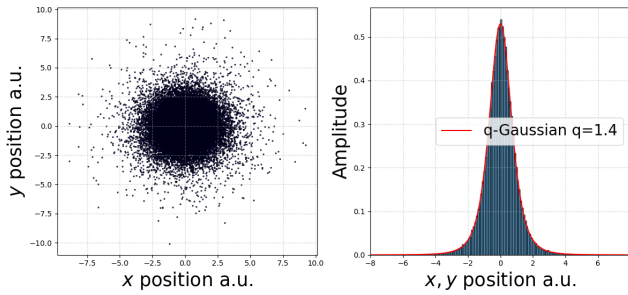


Figure 1: Projection in the  $x - y$ -plane (left) and the  $x$ -plane and  $y$ -plane (right) for a distribution with elliptical symmetry in all planes (case 1).

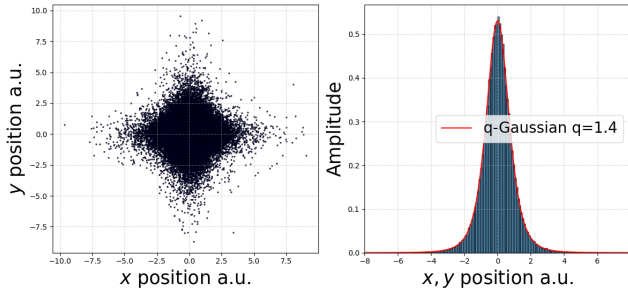


Figure 2: Projection in the  $x - y$ -plane (left) and the  $x$ -plane and  $y$ -plane (right) for a factorizable distribution (case 2).

## APPLICATION TO LUMINOSITY

In the LHC, the luminosity integral is typically calculated assuming factorizable distributions in  $x$  and  $y$ . Below we evaluate the relative luminosity difference for q-Gaussian profiles. We calculate the luminosity for the axis-symmetric distributions as:

$$\mathcal{L} \propto \int_{-\infty}^{\infty} \int_{-\infty}^{\infty} f_{1,2}^2(x, y) dx dy. \quad (23)$$

The integral is done numerically using Eq. (20) for  $f_{1,2}(x, y)$ , replacing  $r_x$  with  $\sqrt{x^2 + y^2}$ .

For factorizable beam distributions we obtain the luminosity as:

$$\mathcal{L} \propto \int_{-\infty}^{\infty} \int_{-\infty}^{\infty} f_{1,2}^2(x) f_{1,2}^2(y) dx dy, \quad (24)$$

where  $f_{1,2}(y)$ ,  $f_{1,2}(x)$  are the q-Gaussian 1D distributions, and 1,2 denotes the two incoming bunches.

Figure 3 shows the luminosity for case 1) and case 2), given the constraint of a q-Gaussian profile in the  $x$  and  $y$  planes, relative to a normal Gaussian distribution. The graph shows as a function of  $q$  a set of q-Gaussian distributions with constant variance and another set keeping  $\beta_q$  constant. The difference in relative luminosity between factorizable and non-factorizable distributions becomes larger as the  $q$ -parameter increases. This shows that it is important to know the properties of the full phase space distribution to accurately calculate the luminosity integrals. For completeness, Fig. 4 shows the q-Gaussians beam profiles (1D projections

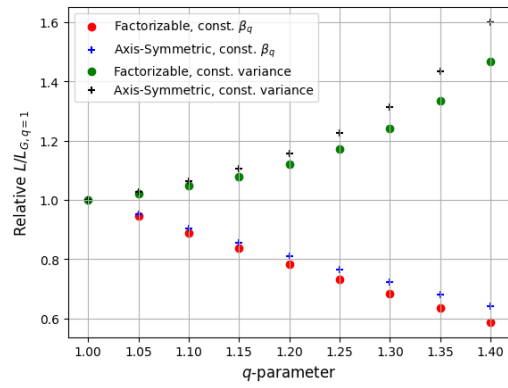


Figure 3: Luminosity variation for different  $q$ , but the same  $\beta_q$  (red and blue markers), and for constant variance (green and black markers), with axis-symmetric (crosses) or factorizable (points) distributions in  $x - y$ .

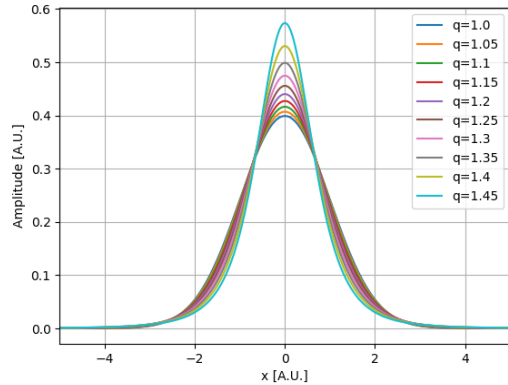


Figure 4: The profile for a q-Gaussian with different  $q$ -parameters for constant variance.

of the phase space) corresponding to the same  $q$ -parameters as of Fig. 3 for the case of constant variance.

The analysis can be extended to include different distributions, correlations, and reconstruction constraints, to see how the crossing angle, luminosity burn-off, and time integrated luminosity are affected depending on the full phase-space distribution. Here we have shown one dependent heavy tail distribution, of which there are infinite.

## CONCLUSION

Given a beam profile, the corresponding 4D phase space distribution is not uniquely defined. Two examples of matched 4D phase space distributions have been reconstructed, one circular symmetric and one factorizable in  $x - y$ , resulting in the same q-Gaussian beam profile. It has been shown that, the resulting luminosity integrals differ depending if the phase space distribution is factorizable in the  $x - y$  plane or not.

## REFERENCES

- [1] E. Lamb *et al.*, "Measurements of beam correlations induced via coupled resonance crossing in the CERN PSB", presented

at the 14th International Particle Accelerator Conf. (IPAC'24), Nashville, Tennessee, USA, May 2024 paper TUPC07, this conference.

- [2] N. H. Abel, "Oeuvres complètes", Christinia, Paris, France, 1881.
- [3] R. Bracewell, "The Fourier transform and its applications, 3rd ed.", McGraw-Hill, New York, 1999.
- [4] Yuri Batygin, "Particle-in-cell code BEAMPATH for beam dynamics simulations in linear accelerators and beamlines", *Nuclear Instruments and Methods in Physics Research Section A: Accelerators, Spectrometers, Detectors and Associated Equipment*, vol. 539, pp. 455-489, Mar. 2005. doi: 10.1016/j.nima.2004.10.029.
- [5] S. Papadopoulou *et al.*, "Impact of non-Gaussian beam profiles in the performance of hadron colliders", *Phys. Rev. Accel. Beams*, vol. 23, no. 10, p. 101004, Oct. 2020. doi: 10.1103/PhysRevAccelBeams.23.101004.
- [6] F. Asvesta *et al.*, "Characterization of transverse profiles along the LHC injector chain at CERN", in *Proc. IPAC'23*, Venice, Italy, May 2023, pp. 3490–3493. doi: 10.18429/JACoW-IPAC2023-WEPL158.
- [7] E M F Curado and C Tsallis, "Generalized statistical mechanics: connection with thermodynamics", *Journal of Physics A: Mathematical and General*, vol. 24, no. 2, p. L69, Jan. 1991. doi: 10.1088/0305-4470/24/2/004.
- [8] G. Box and M. Müller, "A Note on the Generation of Random Normal Deviates", *The Annals of Mathematical Statistics*, 1958. doi: 10.1214/aoms/1177706645.